View metadata, citation and similar papers at core.ac.uk

brought to you by CORE

provided by Elsevier - Publisher Connector

Neuron, Vol. 19, 465–471, September, 1997, Copyright ©1997 by Cell Press

Chemical Two-Photon Uncaging: A Novel Approach to Mapping Glutamate Receptors

Neurotechnique

Diana L. Pettit,[†‡] Samuel S.-H. Wang,[†] Kyle R. Gee,[*] and George J. Augustine
Department of Neurobiology
Duke University Medical Center
Durham, North Carolina 27710
*Molecular Probes
Eugene, Oregon 97402

Summary

Functional mapping of neurotransmitter receptors requires rapid and localized application of transmitter. The usefulness of caged glutamate for this purpose has been limited, because photolysis by unfocused light above and below the target cell limits depth resolution. This problem is eliminated by using a double-caged glutamate that requires absorption of two photons for conversion to active glutamate, resulting in a substantial improvement in spatial resolution over conventional caged glutamate. This method was used to map the distribution of glutamate receptors on hippocampal pyramidal neurons. A higher density of AMPA receptors was found on distal apical dendrites than on basal or primary apical dendrites, suggesting that synaptic efficacy is locally heterogeneous. Such "chemical two-photon uncaging" offers a simple, general, and economical strategy for spatially localized photolysis of caged compounds.

Introduction

Caged compounds are biological signaling molecules inactivated by a photosensitive blocking group. When these compounds absorb ultraviolet (UV) light, a covalent bond attaching the caging group is broken, and an active signaling molecule is released. These compounds are useful tools in studying synaptic transmission, in part because photolysis is rapid and can produce immediate jumps in the concentration of neurotransmitters or second messengers (McCray and Trentham, 1989; Adams and Tsien, 1993; Hess et al., 1995). In addition, this photolysis can be localized by restricting UV light to a small part of the field to yield spatial information about signaling events (O'Neill et al., 1990; Parker and Yao, 1991; Callaway and Katz, 1993; Wang and Augustine, 1995).

One difficulty with spatially resolved uncaging is that when caged compounds are present throughout thick specimens, such as brain slices, even a well focused light beam will cause diffuse photolysis. This occurs because light on its way to and from the focal point will photolyze caged compounds in untargeted tissue. Such conditions yield axial (depth) and lateral resolution on the order of tens of micrometers, even when light is focused to a diffraction-limited spot less than a micrometer wide (Katz and Dalva, 1994; Wang and Augustine, 1995).

Here, we describe an approach to eliminating out-of-focus uncaging of the neurotransmitter glutamate. This approach is based on attaching two caging groups to a single glutamate molecule (Figure 1A), a concept independently proposed by Adams and Tsien (1993). Since each caging group inactivates the glutamate (Wieboldt et al., 1994), both cages must be photolyzed to obtain active glutamate. The resulting requirement for two photons should produce glutamate in proportion to the square of the light intensity and do so primarily at the focal plane. We tested this strategy in hippocampal pyramidal neurons by comparing the performance of a novel double-caged glutamate to that of a single-caged glutamate, and we report that this approach substantially improves depth resolution.

Results

Theory and Predictions

As UV light is focused on a specimen, it passes through a double cone-shaped volume in which glutamate can be produced (Figure 1B). In our microscope, light passes through a multimode optical fiber that transmits an approximately Gaussian light beam that overfills (total possible angle of 64°) the back aperture of a water-immersion objective (numerical aperture of 0.7). The objective emits a truncated Gaussian beam, whose half-maximal width converges at a total angle of about 54° and tapers to a spot 5.6 μm wide and ~15 μm deep (lines in Figure 1C; Wang and Augustine, 1995). From this geometry, we can predict the distribution of photolyzed glutamate within the light beam. Simplifying assumptions about cell geometry and glutamate sensitivity then allow us to estimate cellular responses as a function of axial position within the light beam.

We first assumed that at any given depth z, the light forms a Gaussian spot with half-maximal radius $r_{spot}(z)$. Because the total amount of light is approximately constant in any horizontal cross-section of the beam (e.g., red and blue lines, Figure 1B), peak light intensity at the center of any cross-section must be inversely proportional to the spot area, $r^2_{spot}(z)$; the light energy density per unit area within a given plane in the light beam is then

$$A(r,r_{spot}) = \frac{A_0 2^{-r^2/r^2_{spot}(z)}}{r^2_{spot}(z)}, \quad (1)$$

where r is the lateral distance from the center of the spot and A_0/r^2_{spot} is the light intensity at the center of the spot (Siegman, 1971). For light intensities that photolyze only a small fraction of the caged glutamate—i.e., when the product of $A(r,r_{spot})$, the caged glutamate extinction coefficient, and the quantum yield is much less than 1—the amount of glutamate is linearly proportional to

[†] These authors contributed equally to this work.
[‡] To whom correspondence should be addressed.

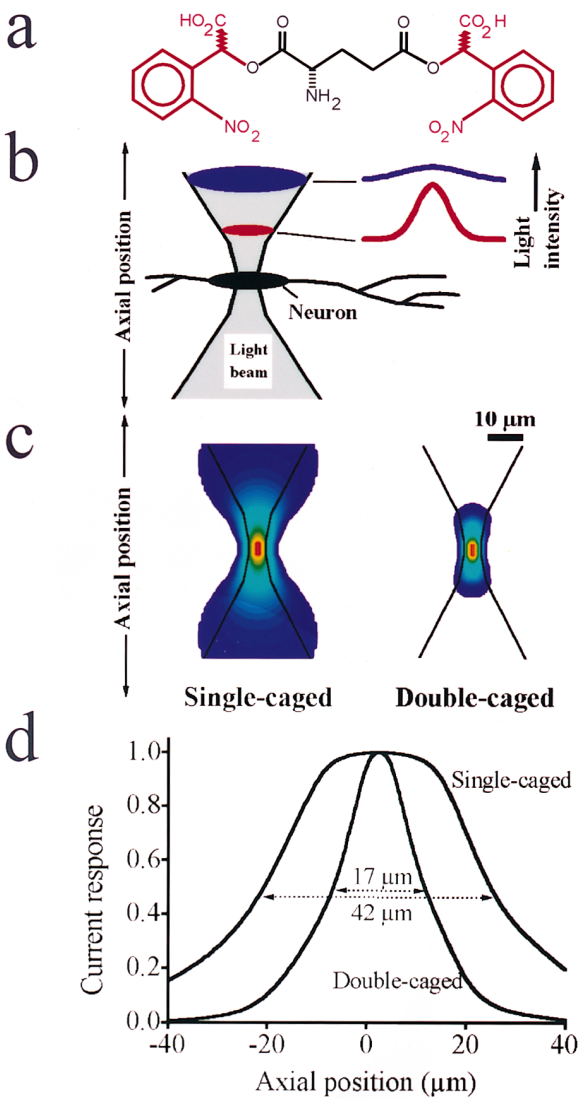

Figure 1. Improvement in Spatial Resolution during Photolysis of Double-Caged Glutamate

(a) Structure of double-caged glutamate.

(b, left) Schematic side view of a UV light beam focused onto a neuron (black). At different horizontal planes (red and blue) the spot contains a constant total amount of light.

(b, right) For each of the cross sections shown on the left, light intensity varies with distance from the center of the beam.

(c) Side view of expected patterns of glutamate production following photolysis of single- and double-caged glutamate. Red indicates the highest concentration and blue the lowest; black lines are experimental measurements of the envelope of the light beam produced by our optical system.

(d) Predicted relationships between the axial position of the light spot and responses to single- and double-caged glutamate.

$A(r,r_{spot})$ and will be distributed as shown in Figure 1C (left).

To predict the cellular response to photolysis of glutamate, we assumed that electrical current, I, is produced in proportion to glutamate concentration (Figure 2B; see also Hausser and Roth, 1997). The response of a neuron to photolysis of single-caged glutamate ($I_{single}[z]$) is then equal to the integral of $A(r,r_{spot})$ over the area of the cell:

$$I_{single}(z) = I_0\, Cp[1 - 2^{-r^2_{cell}/r^2_{spot(z)}}], \quad (2)$$

where C is caged glutamate concentration; p is the probability of photolyzing a single caging group at the center of the focused spot and is proportional to the light flash energy, the extinction coefficient, and the quantum yield; and I_0 is a parameter proportional to the responsiveness of receptors to glutamate. This calculation holds if the flash is briefer than the time required for caged molecules to diffuse out of the light spot; the mean time for a glutamate molecule (diffusion coefficient of 200 $\mu m^2/s$) to escape from the oblong, hourglass-shaped volume shown in Figure 1C is ~10–15 ms (Crank, 1975).

Equation 2 predicts that $I_{single}(z)$ is maximal when the spot radius is smallest. Cellular geometry determines the drop-off of $I_{single}(z)$ with depth; Equation 2 predicts that $I_{single}(z)$ is half-maximal at a cross section where the spot covers an area about as large as the cell. This relationship arises because the quantity of glutamate produced in each horizontal plane is the same, so the response will decline only when the light spot is so large that most of the glutamate in the plane is distant from the cell (blue, Figure 1B). With our conditions (r_{cell} of ~10 μm), Equation 2 predicts that the response of a pyramidal cell will decline to half its maximum over a depth of 42 μm (Figure 1D).

With double-caged glutamate, two photons of UV light are required to produce free glutamate, and the concentration of glutamate produced should be proportional to the square of the flash energy density, $[A(r,r_{spot})]^2$ (Figure 1C, right). This requirement for two photons should greatly reduce the out-of-focus uncaging exhibited by single-caged glutamate (Figure 1C, left). Integrating $[A(r,r_{spot})]^2$ over the cell surface then yields a predicted response of

$$I_{double}(z) = \frac{I_0\, C\, r^2_{\ 0}\, p^2}{2} \frac{[1 - 2^{-2r^2_{cell}/r^2_{spot(z)}}]}{r^2_{\ spot}(z)} \quad (3)$$

where C, p, and I_0 are defined as in Equation 2 and r_0 is the radius of the light spot in the focal plane ($z = 0$). The additional denominator in Equation 3 arises from the square-law relationship and reflects the fact that, when using double-caged glutamate, the total amount of glutamate produced is less at horizontal cross-sections where the light is more diffuse. This denominator also dominates the response profile, so that $I_{double}(z)$ is approximately half-maximal when the spot is twice the size of its most focused area. Thus, for double-caged glutamate, axial resolution depends on the angle of light beam convergence and focused spot size, with resolution optimal when the light beam is wide enough to fill the numerical aperture of the objective.

With nonsaturating light intensities ($p \ll 1$), Equation 3 predicts that in our system (r_0 of 2.8 μm), the expected half-maximal depth for the response to photolysis of double-caged glutamate should be 17 μm (Figure 1D), a 60% improvement in axial resolution over single-caged glutamate. For more intense flashes, the axial resolution of responses is predicted to degrade. Numerical calculations indicate that for $p = 0.9$, the half-maximal depth for double-caged glutamate will expand to 32 μm. This

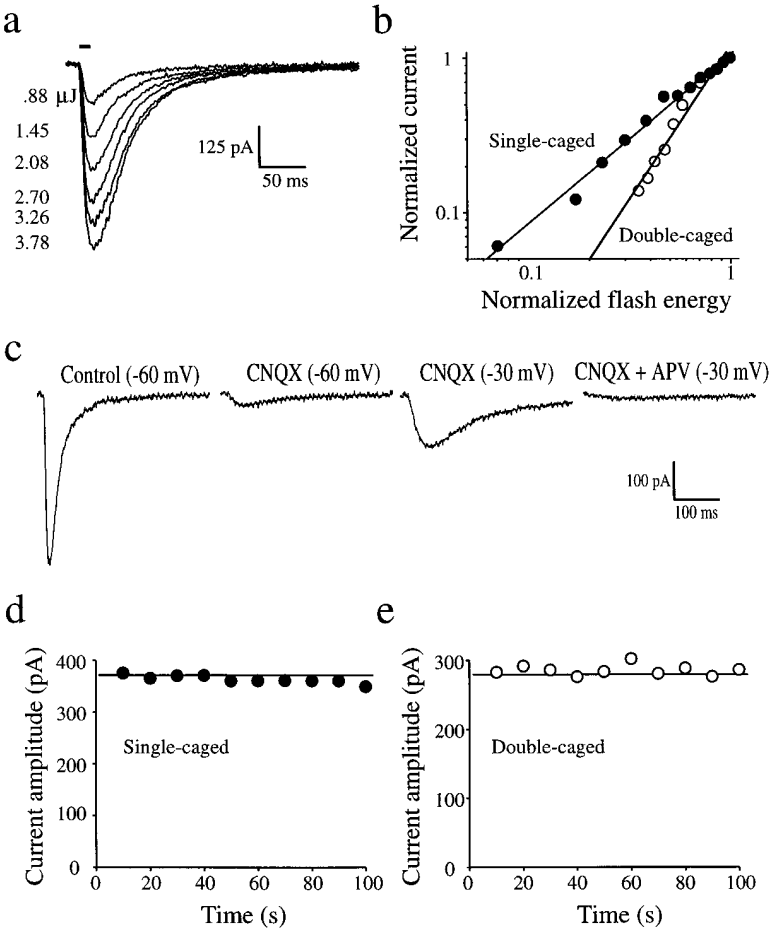

Figure 2. Responses of Pyramidal Neurons to Photolyzed Glutamate

(a) Currents evoked by uncaging single-caged glutamate (50 μM) to differing degrees by varying laser power during 10 ms light flashes (at bar).

(b) Relationship between light energy and peak amplitude of currents evoked in individual pyramidal neurons by single-caged (closed circles) or double-caged (open circles) glutamate. Linear regression fits to the log–log plotted data (solid lines) give slopes of 1.09 for single-caged and 1.97 for double-caged glutamate.

(c) Photolysis of single-caged glutamate induces currents mediated by both AMPA and NMDA receptors. CNQX (5 μM) eliminated most of the current, and the remainder was eliminated by APV (50 μM). Traces are averages of five responses.

(d and e) Stability of currents evoked during repetitive flashes separated by 10 s intervals.

occurs because saturation causes the region of maximal glutamate production to become more distributed.

Treatment of the cell body as a sphere requires numerical integration and predicts a half-depth for single-caged glutamate that is somewhat increased (55 μm) but for double-caged glutamate is nearly the same as for a disk (18 μm). This confirms that depth resolution should be improved substantially through the use of double-caged glutamate and is strongly dependent on detector geometry only for single-caged glutamate.

Experimental Results

Characterization of Responses to Caged Glutamate

Photolysis of either single- or double-caged glutamate over the cell body or dendrite of a pyramidal cell evoked inward currents (Figure 2A). Current responses began 0.3 ms ± 0.1 ms (SEM; n = 13) after the flash and reached a peak at the end of the flash, indicating that glutamate was photolyzed rapidly (Wieboldt et al., 1994) and released throughout the flash. The amplitude of these currents depended upon caged glutamate concentration and light energy (Figure 2B). Responses saturated at ~8 μJ, although we usually confined our measurements to sub-saturating light levels. At these lower light levels, the relationship between light energy and current amplitude evoked by single-caged glutamate was well fit by a first-power relationship (Figure 2B). This is expected if the photolytic release of glutamate requires only a single photon and is consistent with dose-response curves obtained following iontophoretic application of glutamate (Hausser and Roth, 1997). In contrast, for double-caged glutamate, this relationship was nonlinear and could be described by a second-power function (Figure 2B). The observation that this function is the square of the relationship observed for single-caged glutamate supports the idea that two photons are required to produce a molecule of free glutamate.

Currents induced by photolysis of caged glutamate were separated into two components by using glutamate receptor antagonists (Figure 2C; Honore et al., 1988). The most rapid current component was blocked by application of the AMPA receptor antagonist CNQX (5 μM). The remaining current peaked after the end of glutamate production, was enhanced by depolarization to −30 mV, and was blocked by the NMDA receptor antagonist APV (50 μM), consistent with responses mediated by NMDA receptors (Lester et al., 1990). These results show that currents evoked by photolysis of caged glutamate were generated exclusively by activation of AMPA- and NMDA-type glutamate receptors.

At comparable light flashes and concentrations, responses to double-caged glutamate were smaller than those evoked by single-caged glutamate. To compare responses to the two compounds, the concentration of double-caged glutamate was increased until currents

were similar in amplitude to those evoked by single-caged glutamate. Flashes of 5 ms evoked current responses of 72 ± 10 pA (SEM, n = 10) with 25 μM single-caged glutamate and 73 ± 7 pA (n = 8) for 100 μM double-caged glutamate. Doubling the concentration of each compound resulted in response amplitudes that also doubled, to 140 ± 16 pA (n = 10) and 146 ± 17 pA (n = 7). This lowered probability of producing free glutamate is additional evidence that two photons are required to activate double-caged glutamate; since the probability of photolyzing a single caging group (p) is <1, the probability of forming glutamate from the double-caged compound (p^2) must always be less than that of forming glutamate from the single-caged compound.

Photolysis of caged glutamate could cause depletion of caged glutamate or accumulation of free glutamate, single-caged glutamate, or carboxynitrobenzyl groups. To test for such phenomena, flashes were repeatedly applied at the focal plane at 10 s intervals. No changes were observed in the amplitude (Figures 2D and 2E) or time course (not shown) of responses, showing that changes in the chemical environment are minimal on a time scale of 10 s.

Comparison of Axial Resolution

If adding a second caging group to glutamate improves axial resolution in focal photolysis experiments, then the size of current responses evoked by double-caged glutamate should drop off more steeply with axial distance than those evoked by single-caged glutamate (Figures 1C and 1D). We tested this prediction by measuring currents elicited while varying the axial distance between the cell and the focal point of the UV light beam. Figure 3A shows current traces recorded after uncaging either single- or double-caged glutamate. Responses were maximal when the spot was focused on the cell and were smaller with increasing distance between the cell and the focal point. However, the spatial decay of these responses differed for the two compounds; for example, when the UV light was focused 20 μm below the cell, single-caged glutamate evoked a response while double-caged glutamate did not. Thus, adding a second caging group to glutamate does improve axial resolution.

To quantitate axial resolution, we measured the relationship between the peak amplitude of glutamate-induced currents and axial position (Figure 3B). These relationships were described by Gaussian functions, whose half-widths were used as a measure of axial resolution (Figure 3B). The mean half-width of this function was 43.5 ± 1.3 μm (SEM, n = 21) for single-caged glutamate and 18.7 ± 1.1 μm (SEM, n = 18) for double-caged glutamate. This 57% improvement in axial resolution over single-caged glutamate is statistically significant ($p < 10^{-6}$, Student's t test) and is in excellent agreement with the theoretical prediction of 60% shown in Figure 1D.

Our calculations predict that a high probability of photolysis of double-caged glutamate should decrease axial resolution (see Theory and Predictions). We tested this by doubling light energy by increasing flash duration. For double-caged glutamate, this increased mean half-widths from 20.4 ± 1.6 μm to 31.1 ± 3.7 μm (SEM, n = 7; p < 0.02, paired t test), while for single-caged glutamate it did not (n = 7; p > 0.05, paired t test). In contrast, increasing response amplitude by increasing caged compound concentration had no effect upon axial resolution; the mean half-widths for 100 and 200 μM double-caged glutamate were indistinguishable (21.5 ± 2.4 μm SEM, n = 5 and 17.6 ± 1.2 μm SEM, n = 13, respectively). This was also true for single-caged glutamate (44.8 ± 1.7 μm SEM, n = 10 at 25 μM and 43.4 ± 1.9 μm SEM, n = 11 for 50 μM; p > 0.1, Student's t test). Thus, axial resolution is independent of caged glutamate concentration and optimal with limited photolysis of double-caged glutamate.

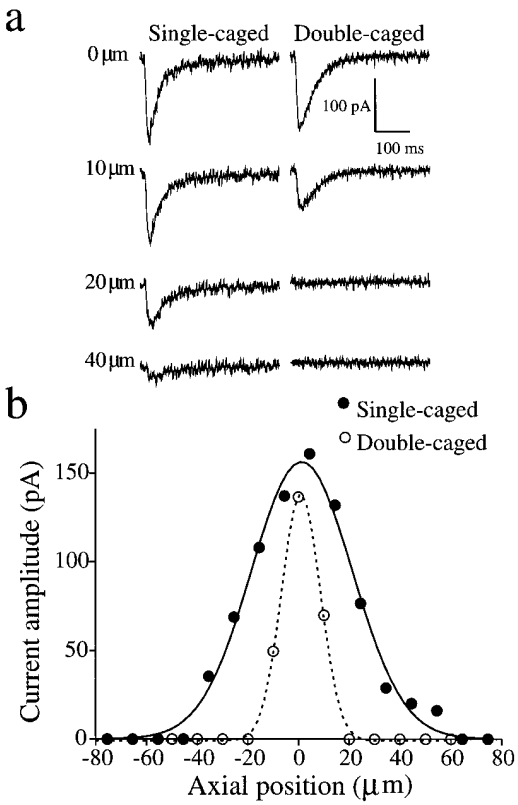

Figure 3. Double-Caged Glutamate Improves Axial Resolution

(a) Current traces evoked by single- and double-caged glutamate (5 ms flashes at 10 s intervals), obtained while varying the distance between the neuronal cell body and the focal plane of the UV light beam.

(b) Relationship between axial position and the peak currents shown in (a). The half-widths of the Gaussian functions fit to single- and double-caged glutamate responses are 40 μm and 15 μm, respectively.

Mapping Glutamate Receptor Distribution

Local uncaging makes it possible to resolve glutamate responses on individual dendrites. We occasionally obtained glutamate responses whose axial profiles had two peaks (Figure 4A) that were fit by the sum of two Gaussians, each of which had a half-width comparable to that seen in single-peaked distributions. Such results may be due to activation of receptors on multiple processes lying in different focal planes. Profiles with multiple peaks were seen with both single- and double-caged glutamate, though peaks <40 μm apart could be resolved only with the double-caged compound.

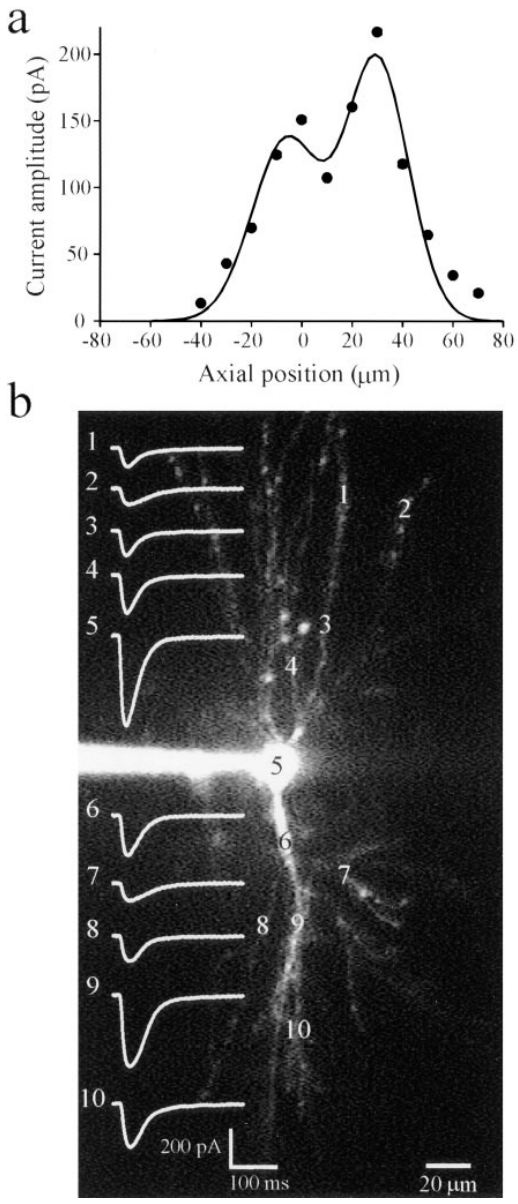

Figure 4. Glutamate Receptor Mapping

(a) A two-peaked relationship between dendritic glutamate responses and axial position using single-caged glutamate. The beam was positioned over a primary dendrite 50 μm from the cell body. (b) Image of a different CA1 pyramidal cell filled with Calcium Green-1. Currents were elicited by photolyzing (3 ms, 1.1 μJ flash) double-caged glutamate (200 μM) at different locations along the cell. Currents were recorded at a holding potential of −60 mV, in the presence of 100 μM cadmium and 1 μM tetrodotoxin.

Local photolysis can be used to map spatial variations in glutamate responses of single neurons by moving the UV light spot to different positions. In such experiments, the lateral resolution was better than 5 μm when using double-caged glutamate, because no current was evoked when the spot was moved 5–10 μm away from a cell. Along the basal dendrite, the amplitude of glutamate-induced currents decreased monotonically as the distance from the cell body increased (compare traces 5, 3, and 1 in Figure 4B). Several mechanisms, including a decrease in receptor density, decreased membrane area exposed to glutamate, or electrotonic attenuation (Spruston et al., 1993), could produce this effect. However, currents were consistently ($n = 5$) larger at distant secondary apical dendrites than at more proximal regions (Figure 4B, currents 6, 9, and 10). These larger currents were not caused by regenerative activation of voltage-dependent channels, because they persisted in the presence of calcium and sodium channel blockers (100 μM cadmium and 1 μM tetrodotoxin). Furthermore, they were not due to NMDA receptor activation, because 50 μM APV did not eliminate the effect. These larger currents apparently reflect a higher density of AMPA receptors in secondary apical dendrites.

Discussion

Using a double-caged glutamate compound, we have achieved a significant improvement in the spatial resolution of focal uncaging in brain slices. The observed improvement in depth resolution, the nonlinear dependence of response amplitudes on flash energy, and the requirement for higher concentrations of double-caged compound all show that two photolysis events are required to generate one active glutamate molecule. We call this phenomenon "chemical two-photon uncaging" to distinguish it from "optical" two-photon excitation (Göppert-Mayer, 1931), in which two long-wavelength photons from an intense, pulsed laser are needed to provide sufficient energy to photolyze a single caging group (Denk et al., 1990; Denk, 1994; Denk et al., 1995). Though we have restricted our attention to glutamate, attractive candidates for double-caging include other neurotransmitters (Hess et al., 1995) and inositol 1,4,5-trisphosphate, which can be inactivated at both its 4- and 5-phosphate positions (Walker et al., 1989). The caged calcium chelator diazo-4 also must be photolyzed twice to cause a maximal shift in calcium affinity (Adams et al., 1988). These possibilities suggest that chemical two-photon uncaging will be a very general method for improving the performance of any compound to which two inactivating caging groups can be attached.

Chemical two-photon uncaging has several advantages over optical two-photon uncaging. (1) Economy. A laser capable of producing the long-wavelength photons necessary for optical two-photon excitation costs ~$100,000 (Denk et al., 1995), while chemical two-photon uncaging can be produced by an argon laser (~$20,000) and may even be obtained with the inexpensive arc lamps found on virtually all fluorescence microscopes. (2) Photolytic efficiency. Relatively little uncaging occurs during optical two-photon excitation because many existing caging groups are not photolyzed efficiently by two long-wavelength photons (Denk et al., 1995). Chemical two-photon uncaging avoids this problem by relying on the UV photolysis for which the compounds were originally designed. (3) Spatial resolution. Because the diffraction-limited point spread is proportional to wavelength (Inoué, 1986), the spatial resolution of chemical two-photon uncaging should be better than that of optical two-photon uncaging, as the former uses shorter-wavelength light. We did not critically test this point in

our experiments, because our UV light was not focused to a diffraction-limited spot. (4) Stability. Spontaneous hydrolysis of single-caged compounds can cause significant amounts of active compound to accumulate in test solutions, leading to unwanted effects, such as toxicity and receptor desensitization. The addition of a second cage to compounds should slow this process; indeed, this appears to be the case for double-caged glutamate (unpublished data).

Chemical two-photon uncaging has several unique requirements. (1) Double-caged compounds. The molecule of interest must have two attachment sites where a caging group will be inactivating. Further, the presence of one caging group must not affect photolysis of the other caging group, as might occur, for example, during resonance energy transfer. Our synthesis of double-caged glutamate was simplified by earlier work identifying multiple sites of inactivation, separated by nonresonant single bonds (Wieboldt et al., 1994). (2) Rapid photolysis. In order for this process to eliminate out-of-focus uncaging, two photons must arrive close enough in time so that the caged molecule cannot diffuse out of the light spot before two photolysis events occur. (3) Lack of saturation. Spatial resolution in local uncaging experiments is maximal when flash-generated glutamate does not saturate receptors and when caged glutamate is not depleted at the focal point.

In summary, double-caged compounds provide a new tool that improves spatially resolved photolysis and makes two-photon uncaging more accessible. With this method, we could resolve local glutamate responses on individual dendritic processes, and we observed indications of higher glutamate receptor density in distal dendrites than in primary dendrites. This could arise from either a higher density of synapses or more receptors per synapse in this region. Whatever their origin, larger responses could weight dendritic inputs or help compensate for electrotonic attenuation. The use of double-caged glutamate and the improvement it brings in spatial resolution will allow further exploration of these and other questions of synaptic function.

Experimental Procedures

Animals

Standard techniques were used to prepare 400 μm thick slices from the hippocampi of 12- to 16-day-old rats (Dingledine, 1984) and to make whole-cell patch clamp recordings from CA1 pyramidal cells. The patch pipette solution contained (in mM): 100 gluconic acid, 2–10 EGTA, 5 $MgCl_2$, 2 ATP, 0.3 GTP, and 40 HEPES (pH to 7.2 with CsOH). Slices were superfused at room temperature with oxygenated physiological saline (in mM: 119 NaCl, 2.5 KCl, 1.3 $MgCl_2$, 2.5 $CaCl_2$, 1 NaH_2PO_4, 26.2 $NaHCO_3$, and 11 glucose) containing 1 μM tetrodotoxin to prevent synaptic transmission and either single- or double-caged glutamate (in DMSO; final concentration, 0.01%). All neurons were voltage clamped at a holding potential of −60 mV and accepted only if the holding current was <100 pA.

Synthesis of Double-Caged Glutamate

A double-caged compound was synthesized by adding a nitrobenzyl caging group to each of the two carboxyl groups of glutamate (Figure 1A). A solution of N-t-butoxycarbonyl glutamic acid (1.03 mM) was alkylated by two equivalents of t-butyl α-bromo-2-nitrophenylacetate (2.06 mM) in benzene:THF (5:2), mediated by 1,8-diazabicyclo{5,4,0}undec-7-ene (DBU; 2.1 mM). The solution was refluxed for 16 hr. The resulting mixture was washed with water and brine, dried with sodium sulfate, and concentrated to a brown syrup. Purification via flash chromatography (Still et al., 1978) gave the intermediate protected bis-ester as 61% of a pale brown oil. By thin layer chromatography (TLC) in 5% EtOAc/$CHCl_3$, the product migrated with an R_f of 0.45. ^1H NMR spectra showed peaks (in $CDCl_3$) at δ (TMS) 8.05 (m, 2H), 7.67 (m, 4H), 7.52 (m, 2H), 6.8 (m, 2H), 5.2 (two t, 1H), 4.5 (br s, 1H), 2.7–2.0 (m, 4H), and 1.4 (m, 27H).

A solution of bis-ester (0.61 mM) in dichloromethane (5 ml) was treated with trifluoracetic acid. The resulting solution was incubated under nitrogen at room temperature in darkness for 16 hr and then concentrated under vacuum. Toluene was stripped from the resulting residue, leaving α,γ-bis-(α-carboxy-2-nitrobenzyl)-L-glutamic acid ester (bis-CNB-, or double-caged glutamate, trifluoracetate salt; Figure 1A) as 95% of a pale yellow powder as the final product. TLC showed an R_f of 0.32 in MeCN:H_2O:AcOH 8:1:1. ^1H NMR peaks (in D_2O) were δ (TMS) 8.10 (m, 2H), 7.82 (m, 2H), 7.70 (m, 4H), 6.7 (m, 2H), 4.4 (m, ^1H), and 3.0–2.2 (m, 4H); and in ^{19}F NMR (D_2O) Φ 71.96. The absorbance at 262 nm gave an extinction coefficient of 7300 $M^{-1}s^{-1}$ at pH 7.0.

Double-caged glutamate spotted on a silica TLC plate was photolyzed for 30 min with a hand-held lamp (254 nm) at a distance of 1 cm. The result was clean production of free glutamate, as judged by coelution of photoproduct with an authentic sample of free glutamate (TLC R_f of 0.10 in MeCN:H_2O:AcOH 8:1:1). We presume that each caged carboxylate group is photolyzed identically to the analogous mono-carboxynitrobenzyl (single) caged glutamates; the α-carboxlyate of single-caged glutamate is photolyzed with a half-life of 80 μs and a quantum yield of 0.16, while photolysis at the γ-carboxylate position occurs with a half-life of 21 μs and a quantum yield of 0.14 (Wieboldt et al., 1994). Double-caged glutamate is hydrophobic and should have less free glutamate contamination than single caged. It should also have less agonist or antagonist activity than single-caged glutamate, which is reported to be biologically inactive at 1 mM (Wieboldt et al., 1994).

Local Uncaging

The output of a continuous emission 5W argon ion laser (Coherent Model 305A, with standard mirrors) was filtered, and 40–80 mW of light at 351 and 364 nm lines was delivered, via a multimode optical fiber, through an Olympus 40× water-immersion objective to form an uncaging spot ~3 μm wide (Wang and Augustine, 1995). Intensity at the front of the objective was 0.1–4 mW, and an electronic shutter (Uniblitz) was used to vary the duration of the light pulse. The uncaging spot was positioned over a cellular process by including fluorescent dye, either fluorescein dextran 10 kDa (30 μM; Molecular Probes, Eugene, OR) or Calcium Green-1 (150 μM; Molecular Probes, Eugene, OR), in the patch pipette solution and then visualizing the cell with a real-time confocal microscope (Noran Odyssey XL).

Acknowledgments

This work was supported by National Institutes of Health grants NS17771 and NS34045, training grant MH15177, and fellowship NS09457. We thank M. B. Dalva, W. Denk, L. L. McMahon, and R. S. Zucker for helpful discussions.

Received May 12, 1997; revised July 24, 1997.

References

Adams, S.R., and Tsien, R.Y. (1993). Controlling cell chemistry with caged compounds. Annu. Rev. Physiol. *55*, 755–784.

Adams, S.R., Kao, J.P.Y., Grynkiewicz, G., Minta, A., and Tsien, R.Y. (1988). Biologically useful chelators that release Ca^{2+} upon illumination. J. Am. Chem. Soc. *110*, 3212–3220.

Callaway, E.M., and Katz, L.C. (1993). Photostimulation using caged glutamate reveals functional circuitry in living brain slices. Proc. Natl. Acad. Sci. USA *88*, 7661–7665.

Crank, J. (1975). The Mathematics of Diffusion, Second Edition (Oxford: Clarendon Press).

Denk, W. (1994). Two-photon scanning photochemical microscopy:

mapping ligand-gated ion channel distributions. Proc. Natl. Acad. Sci. USA *91*, 6629–6633.

Denk, W., Strickler, J.H., and Webb, W. (1990). Two-photon laser scanning fluorescence microscopy. Science *248*, 73–76.

Denk, W., Piston, D.W., and Webb, W.W. (1995). Two-photon molecular excitation in laser-scanning microscopy. In Handbook of Biological Confocal Microscopy, Second Edition, J.B. Pawley, ed. (New York: Plenum), pp. 445–458.

Dingledine, R. (1984). Brain Slices. (New York: Plenum).

Göppert-Mayer, M. (1931). Ueber Elementarakte mit zwei Quantenspruengen. Ann. Phys. *9*, 273.

Hausser, M., and Roth, A. (1997). Dendritic and somatic glutamate receptor channels in rat cerebellar Purkinje cells. J. Physiol. *501*, 77–95.

Hess, G.P., Niu, L., and Wieboldt, R. (1995). Determination of the chemical mechanism of neurotransmitter receptor-mediated reactions by rapid chemical kinetic methods. Ann. N. Y. Acad. Sci. *757*, 23–39.

Honore, T., Drejer, J., Fletcher, E.J., Jacobson, P., Lodge, D., and Nielson, F.E. (1988). Quinoxalinediones: potent competitive non-NMDA glutamate receptor antagonists. Science *241*, 701–703.

Inoué, S. (1986). Video Microscopy (New York: Plenum).

Katz, L.C., and Dalva, M.B. (1994). Scanning laser photostimulation: a new approach for analyzing brain circuits. J. Neurosci. Methods *54*, 205–218.

Lester, R.A.J., Clements, J.D., Westbrook G.L., and Jahr, C.E. (1990). Channel kinetics determine the time course of NMDA receptor-mediated synaptic currents. Nature *246*, 565–567.

McCray, J.A., and Trentham, D.R. (1989). Properties and uses of photoreactive caged compounds. Annu. Rev. Biophys. Biophys. Chem. *18*, 239–270.

O'Neill, S.C., Mill, J.G., and Eisner, D.A. (1990). Local activation of contraction in isolated rat ventricular myocytes. Am. J. Physiol. *258*, C1165–C1168.

Parker, I., and Yao, Y. (1991). Regenerative release of calcium from functionally discrete subcellular stores by inositol trisphosphate. Proc. R. Soc. Lond. [Biol.] *246*, 269–274.

Siegman, A.E. (1971). An Introduction to Lasers and Masers. (New York: McGraw-Hill).

Spruston, N., Jaffe, D.B., Williams, S.H., and Johnston, D. (1993). Voltage- and space-clamp errors associated with the measurement of electrotonically remote synaptic events. J. Neurophysiol. *70*, 781–802.

Still, W.C., Kahn, M., and Mitra, A. (1978). Rapid chromatographic technique for preparative separation with moderate resolution. J. Org. Chem. *43*, 2923–2925.

Walker, J.W., Feeney, J., and Trentham, D.R. (1989). Photolabile precursors of inositol phosphates. Preparation and properties of 1-(2-nitrophenyl)ethyl esters of myo-inositol 1,4,5-trisphosphate. Biochemistry *28*, 3272–3280.

Wang, S.S.-H., and Augustine, G.J. (1995). Confocal imaging and local photolysis of caged compounds: dual probes of synaptic function. Neuron *15*, 755–760.

Wieboldt, R., Gee, K.R., Niu, L., Ramesh, D., Carpenter, B.K., and Hess, G.P (1994). Photolabile precursors of glutamate: synthesis, photochemical properties, and activation of glutamate receptors on a microsecond time scale. Proc. Natl. Acad. Sci. USA *91*, 8752–8756.